Density-functional study of structures and electronic properties of Cd clusters

Jijun Zhao*
Department of Physics and Astronomy, University of North Carolina at Chapel Hill, Chapel Hill, North Carolina 27599-3255
(Received 18 January 2001; published 12 September 2001)

The lowest-energy structures and electronic properties of cadmium clusters are studied by density-functional theory with the generalized gradient approximation. The equilibrium structures of Cd_n ($n=2-21$) clusters are determined from a number of structural isomers, which are generated from genetic algorithm simulations with a tight-binding potential. Various close-packed structures are found for cadmium clusters. Cd_n clusters with $n=4,9,10,15,17,20$ show relatively high stability, which can be related to the electron shell model, and agrees with experimental results. The density of states for the magic number clusters can also be associated with the electronic shell. The theoretical ionization potentials of Cd_n compare well with experimental values. The size evolution of electronic properties from van der Waals to covalent and bulk metallic behavior in Cd clusters is discussed.

DOI: 10.1103/PhysRevA.64.043204 PACS number(s): 36.40.Cg, 36.40.Mr, 73.22.−f

During the past decade, the structural and electronic properties of metal clusters have been intensively studied both theoretically and experimentally [1–4]. It is of fundamental importance to clarify the transition from molecular states to bulk metallic character in metal-atom clusters. In the particular case of divalent metal clusters, such evolution starts from van der Waals–like dimers, in which the atoms have s^2 closed-shell atomic configuration like helium and are only weakly bound. But the bulk solids of these elements are known to be metallic due to the overlap between the *s* and *p* bands. Thus, probing the transition from van der Waals to metallic bonding in divalent metal clusters has been an interesting topic in cluster physics [5–10,23,24].

Among the divalent metal clusters, the cadmium clusters have been much less studied so far. Previous experimental work on Cd clusters includes determination of mass spectrometric abundance, ionization potentials (IPs), and photoelectron spectra [5–7]. In these studies, the effect of electronic shell structures and a rapid transition from van der Waals to metallic behavior have been observed. On the theoretical side, the IPs of Cd_n clusters up to 55 atoms have been described by an empirical tight-binding calculation [8]. Density-functional-theory- (DFT-) based molecular dynamics simulated annealing (SA) within the local density approximation (LDA) has been employed to search the ground state structures of Cd_n with $n \leqslant 20$ [9]. Recently, small Cd clusters up to Cd_6 were calculated using a quantum chemical method with a relativistic large-core pseudopotential and a coupled-cluster correlation [10]. However, there is still no first principles calculation of IPs of Cd_n with $n>6$. Moreover, a comparative study of the cohesion of divalent metal dimers using different density-functional approximations has shown that gradient corrections are significant in determining the ground state properties of these small clusters [11]. Therefore, a comprehensive DFT study with gradient correction of Cd clusters is essential to elucidate the transition from van der Waals clusters toward metallic clusters.

In this work, density-functional electronic structure calculations of Cd_n ($n=2-21$) clusters have been performed using the DMol package [12]. In the DMol calculations, an effective core potential and a double numerical basis including a *d* polarization function (DND) are chosen. The size of the DND basis is comparable to Gaussian 6-31G* basis sets. However, the numerical basis set is much more accurate than a Gaussian basis set of the same size because it has been numerically optimized [12]. The density functional is treated by the generalized gradient approximation (GGA) [13]. The exchange-correlation potential parametrized by Wang and Perdew [14] is used. Self-consistent field calculations are done with a convergence criterion of 10^{-5} a.u. on the total energy and electron density. Geometry optimizations are performed with the Broyden-Fletcher-Goldfarb-Shanno algorithm. We use convergence criteria of 10^{-3} a.u on the gradient and displacement, and 10^{-5} a.u. on the total energy in the geometry optimization.

The SA determination of the cluster global minimal structure based on GGA calculation is rather computationally expensive for Cd_n with $n \geqslant 10$. Alternatively, we generate a number of low-energy structural isomers for each cluster size by using a genetic algorithm [15–17] with a properly fitted tight-binding potential [18]. The structures obtained from the empirical simulations are then fully optimized with DFT to locate the lowest-energy configuration. The essential idea here is to divide the phase space into several regions and find a locally stable isomer to represent each region. Although the energies and structural parameters of these isomers may not be described very accurately by the empirical potential, these minima might make a reasonable sampling of the phase space and can be further optimized by DFT. If there is no significant difference between the DFT and empirical phase space, the global minimal structure at the GGA level should be achieved by this combination of empirical genetic algorithm search and GGA minimization. The validity of the present scheme was checked in the smaller clusters by increasing the number of structural isomers.

The lowest-energy structures obtained from our calculation are presented in Fig. 1 and described in Table I. For the

*Email address: zhaoj@physics.unc.edu

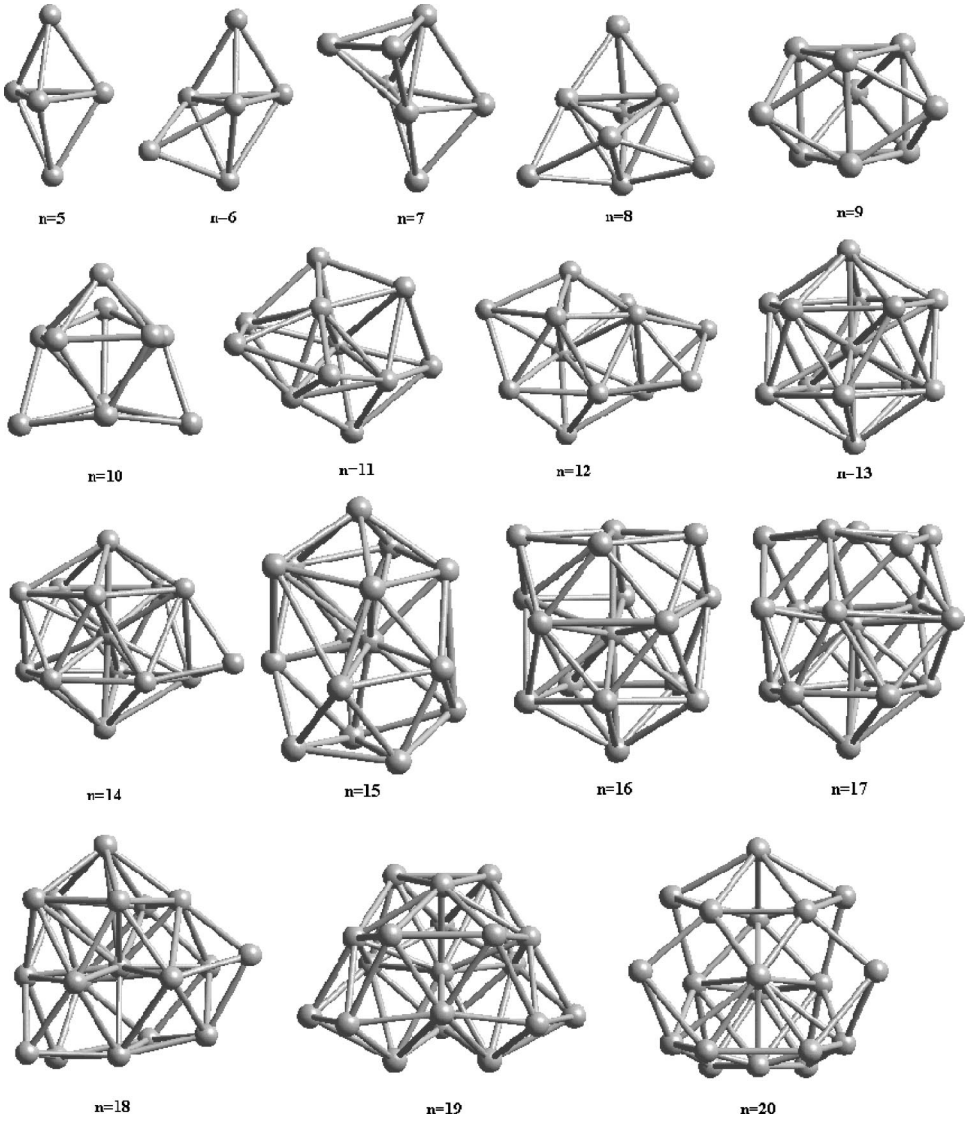

FIG. 1. Lowest-energy structures for Cd_n ($n=5-21$) clusters.

Cd_2 dimer, our GGA calculation predicts the bond length $r=3.29$ Å, binding energy $E_b=0.06$ eV, and vibrational frequency $\omega=56.60$ cm^{-1}. As compared with high-level *ab initio* results (3.96 Å,0.036 eV,20 cm^{-1}) and experimental data (0.039 eV,23 cm^{-1}) [19], the GGA overestimates the binding of the Cd atoms. It is well known that DFT cannot treat van der Waals interactions well. However, as the cluster size becomes larger, the bonding in cadmium clusters will change to covalent or even metallic so that the GGA calculations are expected to describe the cluster properties to a satisfactory extent.

For the cadmium trimer, we find an equilateral triangle structure with bond length 3.45 Å. In the case of Cd_4, the tetrahedron structure with bond length 3.28 Å is lower in energy than a planar rhombus by $\Delta E=0.18$ eV. The lowest-energy structure found for Cd_5 is a trigonal bipyramid. These compact structures of small size, Cd_{3-5}, are the same as the ground state configurations of noble gas clusters [3], implying van der Waals–like bonding in these smallest cadmium clusters. However, the bond length in these small clusters still might be underestimated due to the limit of DFT.

The face-capped trigonal bipyramid is obtained as the lowest-energy structure for Cd_6, while the octahedron structure is 0.17 eV higher in energy. This structure was also obtained as the ground state in a previous LDA-SA simulation [9]. Two isoenergetic structures, a bicapped trigonal bipyramid and a pentagonal bipyramid, are found for Cd_7, with $\Delta E=0.008$ eV. The bicapped tetrahedron has lower energy. It is worth noting that highly symmetrical polyhedrons like the octahedron (O_h) and pentagonal bipyramid (D_{5h}) are predicted for noble gas hexamers and heptamers as ground states [20] but they are energetically unfavorable in Cd_6 and Cd_7. This difference may be attributed to Jahn-Teller instability in the highly symmetrical structures. For example, the HOMO level in Cd_6 with O_h symmetry is doubly degenerate and the molecular level below the HOMO is triply degenerate. All these degeneracies are removed in Cd_6 with the capped trigonal bipyramid (C_{2v}) structure. Therefore, electronic effects start to play an important role in determining the cluster configuration even in small Cd_n clusters down to $n=6,7$.

An additional atom on the bicapped trigonal bipyramid of Cd_7 yields the lowest-energy structure of Cd_8, which is 0.014

TABLE I. Lowest-energy configurations and electronic properties of small Cd_n clusters. BE (eV), binding energy per atom; Δ (eV), gap; IP-I (eV), theoretical direct IP; IP-II (eV), theoretical adiabatic IP; IP-III (eV), experimental IP [5,6].

n	Geometry	BE (eV)	Δ	IP-I	IP-II	IP-III
2	dimer	0.03	3.94	8.09	7.93	7.7
3	equilateral triangle	0.07	3.74	7.80	7.73	7.1
4	tetrahedron	0.13	3.39	7.75	7.75	6.84
5	trigonal bipyramid	0.13	2.86	7.17	6.77	6.68
6	capped trigonal bipyramid	0.14	2.90	7.02	6.95	6.52
7	bicapped trigonal bipyramid	0.15	2.83	6.96	6.39	6.4
8	tricapped trigonal bipyramid	0.17	2.70	6.88	6.30	6.4
9	tricapped trigonal prism	0.19	2.15	6.70	6.34	6.3
10	tetracapped trigonal prism	0.20	1.93	6.28	6.06	5.93
11	interpenetrated pentagonal bipyramids	0.20	2.09	6.39	6.28	5.9
12	interpenetrated pentagonal bipyramids	0.20	1.89	6.25	6.18	5.9
13	icosahedron	0.19	2.10	6.34	6.27	5.9
14	face-capped icosahedron	0.20	1.88	6.22	6.19	5.9
15	uncompleted double icosahedron	0.24	1.69	6.21	6.16	5.87
16	uncompleted double icosahedron	0.24	1.52	5.96	5.88	5.81
17	uncompleted double icosahedron	0.25	1.38	6.01	5.74	5.76
18	close-packed multicage	0.25	0.92	5.76	5.67	5.63
19	close-packed multicage	0.26	0.89	5.67	5.60	5.5
20	close-packed multicage	0.27	1.56	5.86	5.65	5.45
21	close-packed multicage	0.26	0.86	5.78	5.35	5.37

eV lower in energy than the face-capped pentagonal bipyramid. In a previous LDA-SA simulation, a pentagonal bipyramid was obtained for Cd_7 and a face-capped pentagonal bipyramid for Cd_8. These structures are also found in our simulation as metastable isomers with a very small energy difference, i.e., 0.01 eV, from the lowest-energy configuration. Therefore, we argue that the time scale in the previous LDA-SA study may not be sufficient if there are two or more isoenergetic minima in the phase space.

For Cd_9, the ground state structure is a tricapped trigonal prism. Its energy is lower than that of the tricapped octahedron by 0.11 eV. The lowest-energy structure of Cd_{10} can be taken as a tetracapped trigonal prism but with a certain distortion. This structure is energetically more favorable than a pentagonal bipyramid capped with a triangle by 0.08 eV and a tricapped pentagonal bipyramid by 0.16 eV. The lowest structures found for both Cd_{11} and Cd_{12} can be considered as two interpenetrating pentagonal bipyramids capped with one or two atoms. From Fig. 1, the structures of Cd_{11} and Cd_{12} can also be viewed as three interpenetrating pentagonal bipyramids.

Icosahedral structures are found for Cd_n clusters from $n=13$. For Cd_{13}, the energy of an icosahedron with radius 3.41 Å is lower than that of the cuboctahedron by 0.12 eV and that of hcp close packing by 0.16 eV. An additional atom

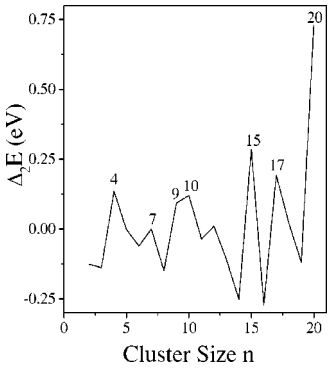

FIG. 2. Second differences of cluster energies $\Delta E(n)=E(n-1)+E(n+1)-2E(n)$ as a function of cluster size n for $n=2-20$. The magic number effect of the electron shell at $n=4,9,10,17,20$ can be identified. See text for details.

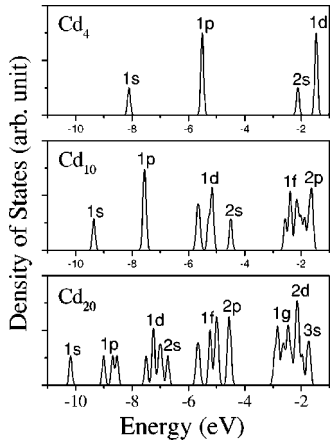

FIG. 3. Density of states of Cd_n ($n=4,10,20$) clusters. Gaussian broadenings of 0.05 eV are used.

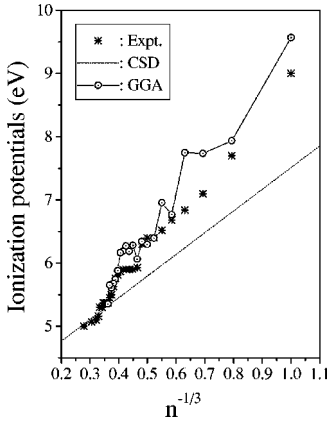

FIG. 4. Ionization potentials vs cluster size n for Cd_n. Stars, experimental data [5,6]; connected open circles, DFT calculations on adiabatic IPs; dashed line, CSD model.

capped on one face of the icosahedron constitutes the lowest-energy structure of Cd_{14}. Cd_{15}, Cd_{16}, and Cd_{17} can be viewed as uncompleted double icosahedrons. However, this structural pattern does not continue at Cd_{18} and the structure of Cd_{19} is not found to be a double icosahedron. Instead, close-packed multicage structures are obtained for Cd_n ($n=18$–21) (see Fig. 1). It is worth noting that 19-atom noble gas clusters have the double icosahedron structure. The current equilibrium structures for Cd_n clusters with $n \geqslant 18$ imply that the bonding in these Cd clusters is quite different from that in van der Waals–like small clusters.

In Fig. 2, we plot the second differences of cluster energies defined by $\Delta_2 E(n)=E(n+1)+E(n-1)-2E(n)$, where $E(n)$ is the total energy of Cd_n clusters from DFT calculations. In cluster physics, $\Delta_2 E(n)$ is a sensitive quantity that reflects the stability of clusters and can be directly compared to the experimental relative abundance. In Fig. 2, maxima are found at $n=4,9,10,15,17,20$. The present results agree with a previous LDA-SA simulation ($n=4,7,10,13,15,17,20$) [9] and experimental mass spectra ($n=10,15,20$) [6,7]. The particularly high stability at Cd_4, Cd_9, Cd_{10}, Cd_{17}, and Cd_{20} might be related to the magic numbers of total valence electrons 8, 18, 20, 34, and 40 predicted by the electronic shell model [1,2]. However, the magic number at Cd_{18} is not obtained from the present calculations although it is observed experimentally [6].

We further investigate the character of the electronic shell in Cd clusters by examining the electronic density of states (DOS). In Fig. 3, we present the electronic DOS for some magic number clusters: Cd_4, Cd_{10}, and Cd_{20}. The energy levels of valence electrons can be identified into groups that correspond to discrete $1s$, $1p$, $1d$, $2s$, $1f$, $2p$, $1g$, $2d$, and $2s$ orbitals in the shell model. In previous studies, the discrete nature of electronic states in cadmium clusters has been observed in the experimental photoelectron spectra and discussed in the framework of the electron shell model based on the jellium approximation [6,7]. The observation of electron shells in Cd_n clusters indicates that Cd_n clusters containing more than a few atoms may already have some metalliclike features that are similar to alkali-metal clusters.

The ionization potential of a metal cluster is one of the most important quantities that can signal the onset of metallic characteristics in the microcluster. For alkali-metal clusters such as Na_n and K_n, the IP converges to its bulk limit (work function of the solid) linearly with $n^{-1/3}$ (or $1/R$, where R is the cluster radius) [2]. Such behavior can be understood by a conducting spherical droplet (CSD) model [20,21], which considers the cluster as a metallic spherical droplet and may also include some quantum effect corrections [21]. For the transition-metal clusters Ni_n, Fe_n, and Co_n [22] and the divalent metal cluster Hg_n [23], the $1/R$ law given by the CSD model breaks down below a certain critical cluster size, i.e., 20–50 atoms, corresponding to the nonmetallic behavior in these small clusters.

In this work, we calculate the ionization potentials from the total energy difference between the ground state neutral Cd_n and the fully relaxed cationic Cd_n^+ clusters. The theoretical results are given in Table I along with the experimental values [5,6]. Satisfactory agreement between theory and experiments is obtained. In Fig. 4, the IPs of Cd_n are plotted as a function of $1/n^{-1/3}$ and compared with the prediction of the classical conducting sphere droplet model [21]. We find that the discrepancy between the CSD model and theoretical or experimental values decreases rapidly as the cluster size increases. As n approaches 20, the discrepancy between DFT calculations and CSD model becomes rather small, indicating that Cd_n clusters with $n \geqslant 20$ become close to a metallic droplet. The size dependence of the IPs of Cd_n clusters is different from that of Hg_n. The transition from van der Waals to covalent and metallic behavior in Cd_n occurs more rapidly than that in Hg_n clusters. For instance, the HOMO-LUMO gap of Cd_n clusters in Table I decreases from 3.94 eV for Cd_2 to 0.86 eV for Cd_{21}, while the band gaps of Hg_3 and Hg_{20} are 3.43 eV and 1.8 eV, respectively [24]. Our present argument is consistent with experiments [5–7].

In summary, we have studied the geometric and electronic structures of cadmium clusters by using a DFT-GGA calculation combined with a genetic algorithm. The main conclusions can be summarized in the following points. (1) Close-packing structures are found for cadmium clusters; electronic effects such as electronic level degeneracy play some role in determining the ground state configurations of Cd_n, which are different from those of noble gas clusters. (2) An electronic shell effect is found from DFT calculations even though the geometrical effect is directly incorporated. Cadmium clusters with closed electronic shells ($n=4,9,10,17,20$) demonstrate the ''magic number'' feature. (3) The size dependence of ionization potentials shows a rapid convergence toward the bulk limit and Cd_n clusters with $n \geqslant 20$ might already be bulk-metallic-like.

This work is partially supported by the U.S. Army Research Office (Grant No. DAAG55-98-1-0298) and NASA Ames Research Center. The author acknowledges computational support from the North Carolina Supercomputer Center.

[1] M. Moskovits, Annu. Rev. Phys. Chem. **42**, 465 (1991).
[2] W.A. de Heer, Rev. Mod. Phys. **65**, 611 (1993).
[3] *Clusters of Atoms and Molecules I*, edited by H. Haberland (Springer-Verlag, Berlin, 1995).
[4] V.V. Kresin and W.D. Knight, Z. Phys. Chem. (Munich) **203**, 57 (1998).
[5] M. Ruppel and K. Rademann, Chem. Phys. Lett. **197**, 280 (1992).
[6] K. Rademann *et al.*, Ber. Bunsenges. Phys. Chem. **96**, 1204 (1992).
[7] K. Rademann, J. Non-Cryst. Solids **156-158**, 794 (1993).
[8] J. Zhao, X. Chen, and G. Wang, Europhys. Lett. **28**, 311 (1994).
[9] F. Yonezawa and H. Tanikawa, J. Non-Cryst. Solids **207**, 793 (1996).
[10] H.J. Flad *et al.*, Eur. Phys. J. D **6**, 243 (1999).
[11] G. Ortiz and P. Ballone, Z. Phys. D: At., Mol. Clusters **19**, 169 (1991).
[12] DMol is a density functional theory package with atomic basis distributed by MSI [B. Delley, J. Chem. Phys. **92**, 508 (1990)].
[13] J.P. Perdew and Y. Wang, Phys. Rev. B **45**, 13 244 (1992).
[14] Y. Wang and J.P. Perdew, Phys. Rev. B **43**, 8911 (1991).
[15] D.M. Deaven and K.M. Ho, Phys. Rev. Lett. **75**, 288 (1995); D.M. Deaven *et al.*, Chem. Phys. Lett. **256**, 195 (1996).
[16] Y.H. Luo *et al.*, Phys. Rev. B **59**, 14 903 (1999).
[17] T.X. Li *et al.*, Phys. Lett. A **267**, 403 (2000).
[18] F. Cleri and V. Rosato, Phys. Rev. B **48**, 22 (1993).
[19] M. Yu and M. Dolg, Chem. Phys. Lett. **273**, 32 (1997).
[20] D.M. Wood, Phys. Rev. Lett. **46**, 749 (1981).
[21] J.P. Perdew, Phys. Rev. B **37**, 6175 (1988).
[22] J. Zhao *et al.*, Phys. Rev. B **50**, 15 424 (1994).
[23] K. Rademann, Z. Phys. D: At., Mol. Clusters **19**, 161 (1991); B. Kaiser and K. Rademann, Phys. Rev. Lett. **69**, 3204 (1992).
[24] R. Busani *et al.*, Phys. Rev. Lett. **81**, 3836 (1998).